DOI:10.1190/segam2020-3413533.1

A semi-quantitative integration of 4D seismic with the reservoir model for monitoring of injected gas volumes in a land carbonate reservoir

Philippe Nivlet, Robert Smith, Andrey Bakulin, EXPEC Advanced Research Center, Saudi Aramco; Rudi Lubbe, GPSD, Saudi Aramco*

Summary

We present a new methodology to integrate 4D seismic data acquired continuously over three years to monitor gas injected in a land carbonate reservoir. A rock physics model is first calibrated from well log data, which is then used to transform reservoir simulation results to 4D synthetic seismic data. We show from this modeling that maximum 4D amplitudes of 6-10% NRMS are strongly impacted by gas thickness, while 4D time-shifts have more complex behavior and cannot be integrated in a simple way into a predictive model. Due to relatively high noise levels in comparison to the expected 4D signal, we show that quantitative models fail to be useful in this situation. Instead, we define a gas detectability threshold from a statistical model between gas thickness and 4D amplitudes, and calibrate a qualitative model of gas detectability depending on noise. This model is used to update in a Bayesian way prior detectability probability maps from the reservoir model, and finally, to update probabilistic gas volume maps from the reservoir model.

Introduction

A major goal of time-lapse seismic is to assist in reservoir history matching, which can be done in either a qualitative (*e.g*., Hodgson *et al*., 2017) or in a quantitative (*e.g*., Tian and McBeth, 2015) way. Among the successful published examples of 4D seismic technology, very few concern land carbonate reservoirs. Stiff reservoir rocks, combined with natural spatial reservoir property variability, can make the low-resolution 4D signal very difficult to interpret. For this particular project, the goal of which was to monitor injected gas plume expansion, additional complications have been highlighted (Bakulin *et al*., 2012, 2016). Challenging near-surface conditions consisting of varying sand thickness, highly variable near-surface velocities, and underlying karsted limestone severely inhibit conventional seismic imaging. In addition, seasonal variations in the near-surface conditions resulting from sand dune migration and climatic effects can lead to high levels of 4D noise that can hinder monitoring. To detect a weak signal in such a noisy environment, a highly repeatable acquisition system was required. To achieve this, receivers were permanently buried at 50-80 meters depth, and a dense 10 x 10 meter vibroseis shot carpet was utilized to ensure sufficient sampling for noise attenuation and to achieve high-fold coverage (Jervis *et al*., 2018). A specialized 4D seismic processing workflow was developed (Smith et al., 2019), resulting in a remarkably low level of background 4D noise (around 2-5% normalized root mean square [NRMS] between surveys acquired during a similar time of year). Even then, interpretation of small 4D signal remains challenging.

In this paper, we present a novel workflow that utilizes 4D seismic amplitudes as well as an estimate of signal uncertainty to update consistently the probabilistic gas thickness maps coming from the history-matched reservoir model. This update happens in four separate steps. First, we define the gas detectability as a function of the 4D noise. Next, the prior gas detectability is calculated from the reservoir model. Then it gets updated with the 4D information, and finally, the probabilistic volumetric maps are updated. The full workflow relies on a rock physics model, which is described first.

Simulating 4D response using reservoir model

In the present study, the rock physics model consists of two parts: dry rock moduli are calibrated to porosity using power law or exponential statistical models. The fluid substitution is controlled by Gassmann's equation assuming that the reservoir fluid mix (oil + gas + water) is homogeneous. This model is then used to transform porosity, pressure and fluid saturation from reservoir model to acoustic impedance volumes. Finally, post-stack synthetic seismic is generated by 1D convolution of the resulting reflectivity with the wavelet extracted from real seismic data. The synthetic 4D data are the different amplitude volumes between the current baseline snapshot before the start of gas injection. Once

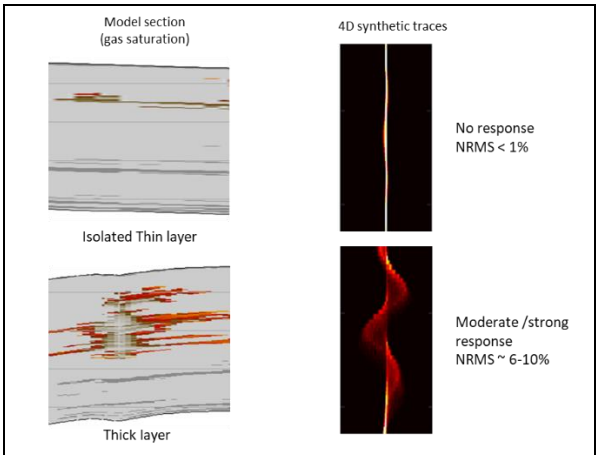

Figure 1. Sections from the 3D gas saturation model (left) and associated 4D amplitude responses (right).

DOI:10.1190/segam2020-3413533.1

calibrated to available well logs, the model is used to transform results from the history matched reservoir model (grids with porosity, facies, fluid saturation, pressure, and temperature) to 4D amplitude volumes. Two types of attributes are then extracted as in Huang *et al*. (2018). Figure 1 shows that as the gas column thickens, amplitude NRMS increases as a result of 4D tuning. A maximum of 6-10% NRMS occurs when the column is fully saturated with gas. The effect of gas on the 4D time shift is more complex and therefore difficult to integrate into a predictive model (Figure 2). If a thickening of the column globally pushes down the 4D amplitude anomaly (yellow vs. green trace), the position of the gas plume in the reservoir can also play an important role (red vs. yellow trace).

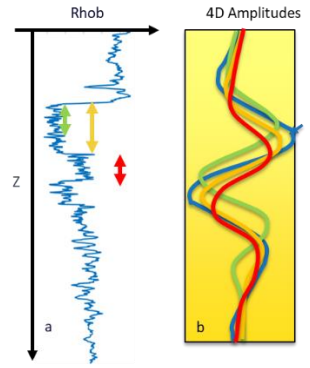

Figure 2. (a) Density log with saturation profile scenarios (red, green yellow); (b) corresponding magnified 4D amplitude traces in comparison with a baseline seismic trace (blue) before injection.

Quantitative seismic volume estimation

A linear model is calibrated between 4D synthetic amplitudes and the corresponding vertical cumulative gas thickness for every time step of the reservoir model. Figure 3a displays a cross-plot between expected and predicted thicknesses using this model. Points are scattered along the first bisector line, indicating that the model is unbiased. The distribution of data along the y-axis represents the prediction uncertainty, from which we can estimate a 95% confidence interval (in yellow). For small thickness values, we observe that this confidence interval spreads to unphysical negative values, meaning the model is unpredictive in this case. We define the minimal detectable gas thickness (MDGT) as the maximal thickness where the prediction confidence interval includes negative values. In Figures 3b and 3c, we have repeated the same calibration exercise, but this time have added respectively 5% and 10% of bandlimited random noise to the 4D traces. As NRMS noise increases, both prediction confidence interval width and MDGT increase, as reflected by Figure 3d. At a level of 5% NRMS noise, we observe that the quantitative model is hardly predictive. This noise level is not unusual in our experiment, as shown, for instance, in Smith *et al*. (2019), especially for surveys acquired during the rainy season. Therefore, we decide not to use this quantitative model directly. Instead, we define a qualitative gas detectability model.

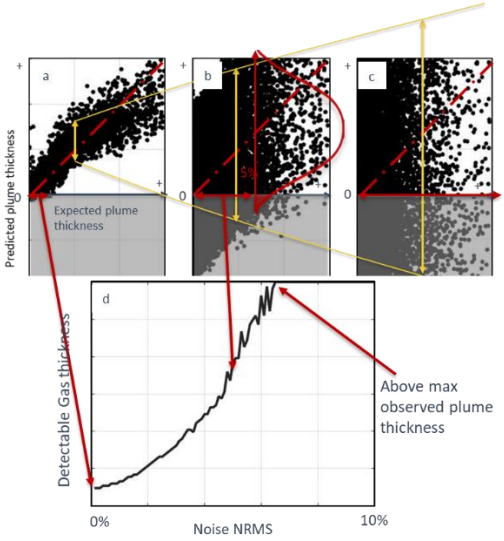

Figure 3. Cross-plots between predicted and expected gas thickness from synthetic 4D amplitudes with 0% (a), 5% (b), and 10% (c) NRMS noise. Variations of MDGT with noise are shown in (d).

Qualitative gas detectability from noisy seismic data

Starting back from the same set of synthetic 4D amplitude maps used to generate Figure 3a, we aim to discriminate between two classes - gas thickness above and below the MDGT. We use a discriminant analysis algorithm for this purpose as proposed by Fournier and Derain (1995) for 3D data interpretation or by Lucet and Fournier (2001) for 4D interpretation. Figure 4a shows that the two classes are well separated in the considered 4D attribute space. Proportions of true positives and true negatives are 75% and 100%, respectively, indicating good discrimination between detectable and nondetectable gas. As 4D noise increases (Figures 4b and 4c with, respectively, 5% and 10% NRMS noise), classes overlap, and the proportions of true positives and true negatives globally decrease as shown in Figure 4d. In addition to accounting for 4D noise during the calibration of this classification function, we also have to account for it for prediction. To do so, Nivlet *et al*. (2001) proposed to generalize the discriminant analysis to interval-valued 4D seismic amplitudes accounting for the 4D noise, resulting in interval-valued probability maps. Here, we propose a simpler approach. 4D noise is represented as a multivariate Gaussian PDF *q*, with zero mean and a diagonal covariance matrix representing the estimated local variance of 4D noise, estimated from a window above the reservoir where no

10.1190/segam2020-3413533.1

physical change is expected between surveys. Figure 5 describes the noise computation process and resulting maps for two survey combinations. The first map exhibits a much higher noise level because the baseline and monitor were acquired under different seasons. On the second map, where baseline and monitor are acquired during similar seasons, noise is moderate. Only in the NE corner is it a bit higher due to lower trace fold.

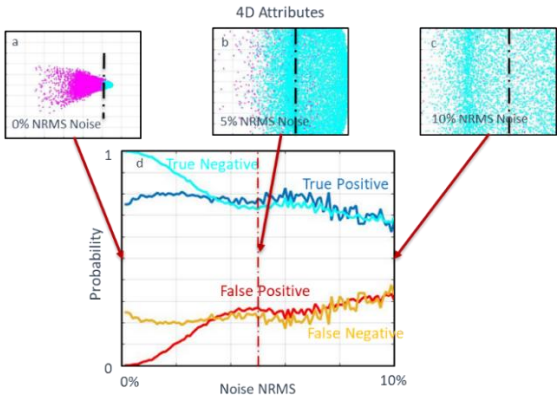

Figure 4. Cross-plots showing detectable and non detectable gas thickness from synthetic 4D amplitudes with 0% (a), 5% (b) and 10% (c) NRMS noise. Plot (d) shows the variation of true and false positves / negatives with noise NRMS associated with the calibrated classifier with linear discriminant analysis.

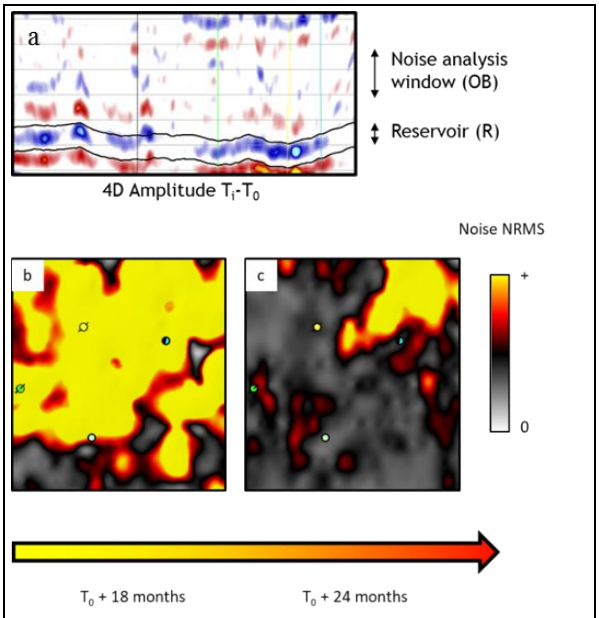

Figure 5. (a) Random line showing 4D amplitudes between two surveys and examples of 4D noise RMS maps estimated at the reservoir level for two different surveys; (b): T_0 + 18 months, and (c): T_0 + 24 months.

This noise is combined with the class probability density functions p derived from the discriminant analysis described above (Equation 1):

$$E[p(x/C_i)] = \int_{x_0} p(x_0/C_i)q(x_0)dx_0. \quad (1)$$

Resulting estimated detectable/nondetectable class probabilities tend to be closer to 0.5 when 4D noise increases.

Figure 6 shows the impact of 4D noise on the predicted class probability. Figures 6a and 6b correspond to the detectable gas probability estimated without accounting for the noise, while Figures 6c and 6d are based on the application of Equation 1. For the (T_0 + 24)-month survey, where noise is moderate, gas detectability is impacted moderately by noise. Conversely, for the (T_0 + 18)-month survey, where 4D noise is very high, detectability probabilities remain between 0.4 and 0.6 almost everywhere, in comparison with the estimated map without noise model where the detectable gas probabilities are overestimated.

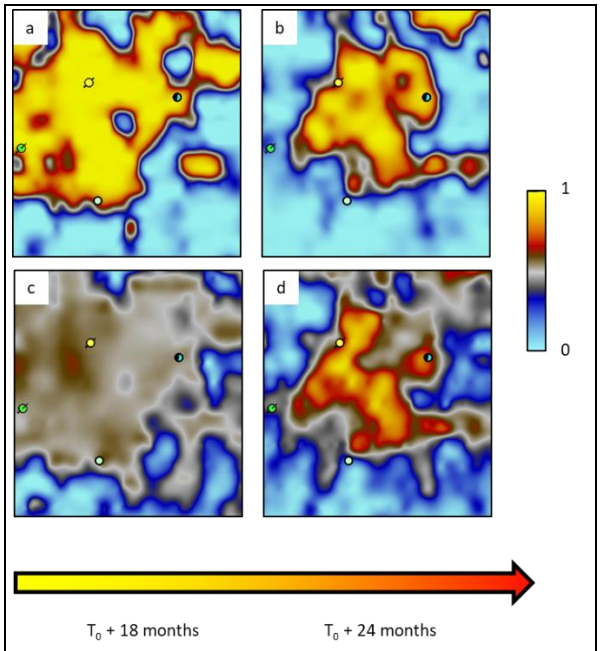

Figure 6. Gas detectability probability from seismic without (a)-(b) and with (c)-(d) accounting for 4D noise; (a)-(c) refer to T_0 + 18 months, and (b)-(d) to T_0 + 24 months.

Prior gas detectability and update with 4D seismic

In the case where we dispose of equiprobable reservoir model realizations from a stochastic process, prior gas thickness uncertainty would be directly estimated from the span of the different realization. In the current study, we did

not dispose of such stochastic models, and instead, we have assumed a prior thickness uncertainty model associated with the cumulated gas thickness estimated from the reservoir model, consisting of a normal distribution and constant thickness standard deviation. By comparing the prior thickness distributions to the local MDGT corresponding to the local noise level, we obtain prior gas detectability maps, as shown in the first row of Figure 7. As expected, the prior detectability for the first survey is generally low, due to a higher noise level (and therefore a higher detectability level). The update of these probabilities is done in two steps. First, Bayes rule is used to compute an intermediate updated probability according to the system of equations (2):

$$(2)\quad \begin{cases} p(v^+/4D^+) = \dfrac{p(v^+)}{p(v^+)+[1-p(v^+)]\frac{p(4D^+/v^-)}{p(4D^+/v^+)}} \\ p(v^+/4D^-) = \dfrac{p(v^+)}{p(v^+)+[1-p(v^+)]\frac{p(4D^-/v^-)}{p(4D^-/v^+)}} \\ p(v^-/4D^+) = \dfrac{1-p(v^+)}{1-p(v^+)+p(v^+)\frac{p(4D^+/v^+)}{p(4D^+/v^-)}} \\ p(v^-/4D^-) = \dfrac{p(v^+)}{1-p(v^+)+p(v^+)\frac{p(4D^-/v^+)}{p(4D^-/v^-)}} \end{cases}$$

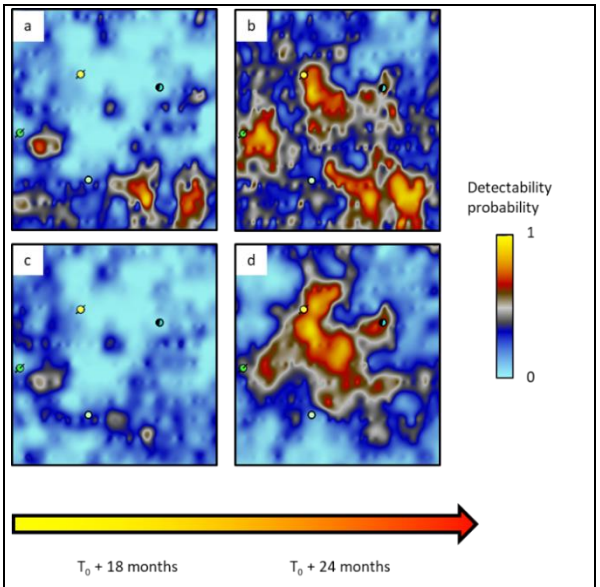

Figure 7. Prior (a and b) and posterior (c and d) gas detectability probability; (a)-(c) refer to T_0 + 18 months and (b)-(d) to T_0 + 24 months

where the *p(v+ or -)* are the prior gas detectability probabilities discussed above; the *p(4D+ or - | v+ or -)* terms are the true/false positives/negatives proportions corresponding to the local 4D noise Figure 4). In the second step, these probabilities are combined with probability maps shown Figures 6c and 6d, using the total probability axiom. Resulting updated maps of gas detectability probability are shown on the Figures 7c and 7d. For the (T_0 + 18)-month survey, seismic has almost no impact on the detectability probability, while the probability map for the (T_0 + 24)-month is heavily modified driven by lower uncertainties in the 4D data.

Prior and updated gas thickness

Finally, to update gas thickness cumulated probabilities (Figures 8e and 8f), we scale the parts of the curve separately above and below the MDGT according to the updated detectability probability. The volumes on Figure 8e are shifted to higher values due to high 4D seismic amplitudes and low associated uncertainties. The volumes Figure 8f are shifted to low values due to low 4D seismic amplitudes and low associated uncertainty. Conversely, volume distributions for most points from the (T_0 + 18)-month survey are not updated due to the high MDGT. Maps shown in Figure 8a to 8d are the Q50 statistics extracted from the local thickness distributions.

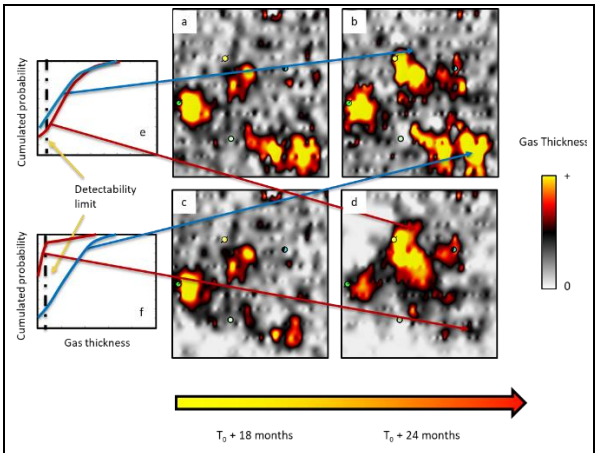

Figure 8. Prior (a)-(b) and posterior (c)-(d) Q50 gas thickness maps; inserts (e) and (f) show two examples of complete prior (blue) or posterior (red) cumulated gas thickness distributions.

Conclusions

We have demonstrated an integrated interpretation of 4D seismic to monitor gas plume expansion in a land carbonate reservoir. 4D nonrepeatability is a critical problem to be addressed since it can heavily bias quantitative seismic interpretation if not accounted for. In this paper, we have shown that by evaluating and propagating 4D noise through the interpretation workflow, we obtain a more consistent picture of the changes occurring in the reservoir. Even though 4D noise is generally too high to have a meaningful quantitative thickness prediction, we can still consistently update volume probabilities using a semi-quantitative model described in the paper.

REFERENCES

Bakulin, A, R. Burnstad, M. Jervis, and P. Kelamis, 2012, Evaluating permanent seismic monitoring with shallow buried sensors in a desert environment: 82nd Annual International Meeting, SEG, Expanded Abstracts, 1–5.

Bakulin, A., R. Smith, M. Jervis, C. Saragiotis, E. Al-Hemyari, and A. Alramadhan, 2016, Processing and repeatability of 4D buried receiver data in a desert environment: 86th Annual International Meeting, SEG, Expanded Abstracts, 5406–5410, doi: https://doi.org/10.1190/segam2016-13849971.1.

Hodgson, L., M. Ball, S. Fowler, M. Gherasim, T. Hance, A. Toomey, and J. P. van Gestel, 2017, Generating value from 4D through efficient integration: The Leading Edge, **36**, 401–406, doi: https://doi.org/10.1190/tle36050401.1.

Fournier, F., and J.-F. Derain, 1995, A statistical methodology for deriving reservoir properties from seismic data: Geophysics, **60**, 1437–1450, doi: https://doi.org/10.1190/1.1443878.

Huang, F., P. Bergmann, C. Juhlin, M. Ivandic. Luth, A. Ivanova, T. Kempka, J. Henninges, D. Sopher, and F. Zhang, 2018, The first post-injection seismic monitor survey at the Ketzin pilot CO2 storage site: Results from time-lapse analysis: Geophysical Prospecting, **66**, 62–84, doi: https://doi.org/10.1111/1365-2478.12497.

Jervis, M., A. Bakulin, and R. Smith, 2018, Making time-lapse seismic work in a complex desert environment for CO2 EOR monitoring—Design and acquisition: The Leading Edge, **37**, 598–606, doi: https://doi.org/10.1190/tle37080598.1.

Lucet, N. and F. Fournier, 2001, 4D data interpretation through seismic facies analysis: 71st Annual International Meeting, SEG, Expanded Abstracts, 1640–1643, doi: https://doi.org/10.1190/1.1816430.

Nivlet, P., F. Fournier, and J.-J. Royer, 2001, A new methodology to account for uncertainties in 4D seismic interpretation: 71st Annual International Meeting, SEG, Expanded Abstracts, 1644–1647, doi: https://doi.org/10.1190/1.1816431.

Smith, R., E. Hemyari, A. Bakulin, and A. Alramadhan, 2019, Making seismic monitoring work in a complex desert environment—4D processing: The Leading Edge, **38**, 637–645, doi: https://doi.org/10.1190/tle38080637.1.

Tian, S. and C. McBeth, 2015, An engineering-consistent Bayesian scheme for 4D seismic to simulator inversion: 77th Conference and Exhibition, EAGE, Proceedings, WS02-C03, doi: https://doi.org/10.3997/2214-4609.201413159.